Farzan, Afsoon; Borandeh, Sedigheh; Baniasadi, Hossein; Seppälä, Jukka

Environmentally friendly polyurethanes based on non-isocyanate synthesis

Published in:
Express Polymer Letters

DOI:
10.3144/expresspolymlett.2024.7

Published: 01/01/2024

Document Version
Publisher's PDF, also known as Version of record

Express Polymer Letters Vol.18, No.1 (2024) 88–101
Available online at www.expresspolymlett.com
https://doi.org/10.3144/expresspolymlett.2024.7

Research article

Environmentally friendly polyurethanes based on non-isocyanate synthesis

*Afsoon Farzan, Sedigheh Borandeh, Hossein Baniasadi, Jukka Seppälä**

Polymer Technology, School of Chemical Engineering, Aalto University, Kemistintie 1, 02150 Espoo, Finland

Received 14 August 2023; accepted in revised form 16 October 2023

Abstract. A series of environmentally friendly non-isocyanate polyurethanes (NIPUs) was synthesized through a polycondensation reaction of as-synthesized semi-bio-based bis-cyclic carbonate with diamine derivatives. The synthesis of bis-cyclic carbonate was realized, for the first time, from 1-thioglycerol and polyethylene glycol diacrylate *via* thiol-ene click and transcarbonation reaction, respectively. The impacts of using different diamine derivatives on the chemical structural, mechanical properties, thermal stability, and surface wettability of the NIPUs were determined. It was found that the NIPU containing fatty acid-based diamine decomposed at a lower temperature than that of other polymers. Besides, it demonstrated a lower Young's modulus and a higher tensile strain at break, possibly due to its four-branched structure and greater flexibility. Meanwhile, the NIPU prepared with *p*-xylylenediamine provided the highest decomposition temperature, owing to an aromatic moiety in the polymer's backbone, which improved its stiffness and thermal stability. Furthermore, it was understood that the NIPU containing diamino-*N*-methyldipropyl-amine exhibited a higher Young's modulus and a lower tensile strain at break, as it had a nitrogen atom in its structure and a trigonal pyramidal configuration with the highest density of hydrogen bonds between polymer chains. Most of the developed NIPUs displayed hydrophobic surface properties, offering promising alternatives to isocyanate-based coating materials.

Keywords: *isocyanate-free polyurethane, structure-property correlation, cyclic carbonate, thermal stability, mechanical properties*

1. Introduction

Over the last decades, replacing hazardous chemicals and dangerous reactions with more environmentally friendly materials and procedures has gained considerable attention. Polyurethanes (PUs), widely used materials in various industries such as chemical, automotive, aerospace, textile, and tissue engineering, are traditionally produced by step-growth addition polymerization between polyols and diisocyanates [1–4]. Isocyanates are very sensitive to moisture, and if moisture is present, a side reaction occurs during the conventional synthesis of PUs in which isocyanate groups may react with water, forming amine and carbon dioxide rather than PU [5]. More importantly, the use of isocyanate is causing environmental and health issues due to its severe toxicity. Furthermore, phosgene is required to synthesize isocyanates, which is a highly toxic, lethal, and energy-intensive gas. Phosgene can cause serious diseases such as pulmonary edema. Besides, this method produces a significant amount of hydrochloric acid as a side product [6–9].

Nowadays, the isocyanate-free method has been considered as an alternative to isocyanate-based routes in the synthesis of polyurethanes. This approach, which is environmentally friendly and reduces the environmental footprint, not only meets sustainable development assumptions but is also part of the current trend of green chemistry [10]. Non-isocyanate polyurethanes (NIPUs) can be synthesized through

*Corresponding author, e-mail: jukka.seppala@aalto.fi

different procedures, including polycondensation, polyaddition, ring-opening polymerization, and rearrangement. From these, the polyaddition of multifunctional cyclic carbonates and primary diamines or polyamines has been considered the most common procedure for synthesizing NIPUs with potential industrial importance [11–13]. NIPU, also known as polyhydroxyurethane (PHU), is synthesized through this reaction, which is also known as aminolysis of cyclic carbonates and consists of pendant hydroxyl moieties with intermolecular hydrogen bonding. Thus, the product may show enhanced thermal stability, elevated mechanical properties, reduced susceptibility to hydrolysis, and increased chemical resistance [14–16].

So far, various cyclic carbonates, from 5-membered to 8-membered cyclic carbonates, have been synthesized for developing NIPUs. Although the reactivity of 5-membered cyclic carbonates is less than the other group members, unlike them, the synthesis of 5-membered cyclic carbonate does not involve hazardous chemicals. So, it is still considered ideal to produce NIPU [8, 17]. Several methods have been used to synthesize 5-membered cyclic carbonates, most of which are based on epoxide or diol reactants [18]. In the former case, 5-membered cyclic carbonates are obtained by combining CO_2 with epoxides. This method has the benefit of using CO_2, which is non-toxic, abundant in nature, chemically inert, and renewable. Furthermore, it can significantly reduce greenhouse gas emissions by combining epoxides with CO_2, making it suitable for synthesizing environmentally friendly cyclic carbonates [19–22]. The epoxidation of unsaturated bonds that are present in the fatty acid chains is a green and sustainable approach for developing bio-based epoxide. As such, some renewable cyclic carbonates from isosorbide, tannins, vanillin, cashew nut shell liquid, limonene, lignin derivatives, and glycerol were described in NIPU synthesis [23, 24]. However, the synthesis of cyclic carbonates through CO_2 chemical fixation has been limited by disadvantages such as high pressures and temperatures, high catalyst loadings, low catalyst stability, and cost-effectiveness [25]. Recently, the transesterification of 1,2-diols, *e.g.*, ethylene glycol, 1,2-propanediol, and glycerol with dialkyl carbonates, *i.e.*, dimethyl or diethyl carbonate, has been considered as an environmentally friendly approach for the cyclic carbonates development. This mild and eco-friendly approach is entropically driven by forming the 1,3-dioxolan-2-one heterocycle (cyclic carbonate) [26]. Thus, we are motivated in the present work to employ this reaction to develop an alternative precursor for epoxides in synthesizing cyclic carbonate monomers.

To this aim, in this study, a novel semi-bio-based cyclic carbonate was first designed and developed using thioglycerol and poly(ethylene glycol) diacrylate (PEGDA) as starting materials. PEGDA is a hydrogel and safe material and is extensively used in tissue engineering applications [27, 28]. Furthermore, thioglycerol, a bio-based material derived from glycerol, is widely used in pharmaceutical and cosmetic formulation, the polymer industry as a stabilizer, and leather processing [29, 30]. A series of NIPUs was synthesized through a polyaddition between the newly developed bis-cyclic carbonate and six different types of diamines. The diamines used in this study had various structures, containing aliphatic chains with different chain lengths, aromatic moieties, and hetero atoms, as well as a branched and fatty acid-based diamine. Here, the main goal was to investigate the relationship between the structure of monomers and the properties of NIPUs. Thus, the synthesized monomers and NIPUs were structurally characterized using different techniques, including FTIR and 1H-NMR. Furthermore, the thermal and mechanical properties of the synthesized NIPUs were evaluated to show their potential for isocyanate-based PU alternatives.

2. Experimental

2.1. Materials

Poly(ethylene glycol) diacrylate (PEGDA, M_n = 250), 1-thioglycerol ≥97%, 2.2-dimethoxy-2-phenylacetophenone (DMPA, 99%), cystamine dihydrochloride (Cys, ≥98%), 3,3′-diamino-*N*-methyldipropyl-amine (DMDPA, 96%), *p*-xylylenediamine (PXD, 99%), triethylamine (TEA, ≥99.5%), dimethyl sulfoxide (DMSO), potassium carbonate (K_2CO_3), *N*,*N*-dimethylformamide (DMF, 99.8%), hexamethylenediamine (HMDA, 98%), diethyl ether, methanol, and dimethyl carbonate (DMC) were purchased from Sigma-Aldrich. 1,10-diaminodecane (DAD, 98%) was obtained from Tokyo Chemical Industry Co (TCI). In addition, priamine™ 1075 (FADA), which is a fatty acid diamine, was kindly provided by CRODA®. All chemicals were used as received.

2.2. Tetraol synthesis

A solution of 20.25 ml poly(ethylene glycol) diacrylate (90 mmol) in 25 ml methanol was prepared in a glass bottle. Then, 15.54 ml 1-thioglycerol (180 mmol) was added gradually at room temperature, and the mixture was stirred for 5 min. After that, 225 mg DMPA (1 wt% to PEGDA) was added as the photoinitiator, and the mixture was exposed to UV light (λ = 365 nm) for 1 h. Finally, the mixture was washed twice with diethyl ether to remove unreacted materials, and the remaining diethyl ether was removed by a rotary evaporator to obtain a clear viscose tetraol product. The reaction between thioglycerol and PEGDA is schematically illustrated in Figure 1.

2.3. The synthesis of bis-cyclic carbonate

Bis-cyclic carbonate was synthesized through the transcarbonation reaction shown in Figure 1b. First, 10 g tetraol (21 mmol) was dissolved in 8.8 ml DMC (105 mmol), and the temperature was raised to 80 °C. Then, 290 mg K_2CO_3 (10 wt% to tetraol) was added as a catalyst. The system was continuously stirred for 72 h to complete the reaction. The yellowish mixture was precipitated in methanol, washed twice, and dried in a vacuum oven.

2.4. Non-isocyanate polyurethane (NIPU) synthesis and film preparation

Non-isocyanate polyurethanes (NIPUs) were synthesized by reacting with as-prepared bis-cyclic carbonate

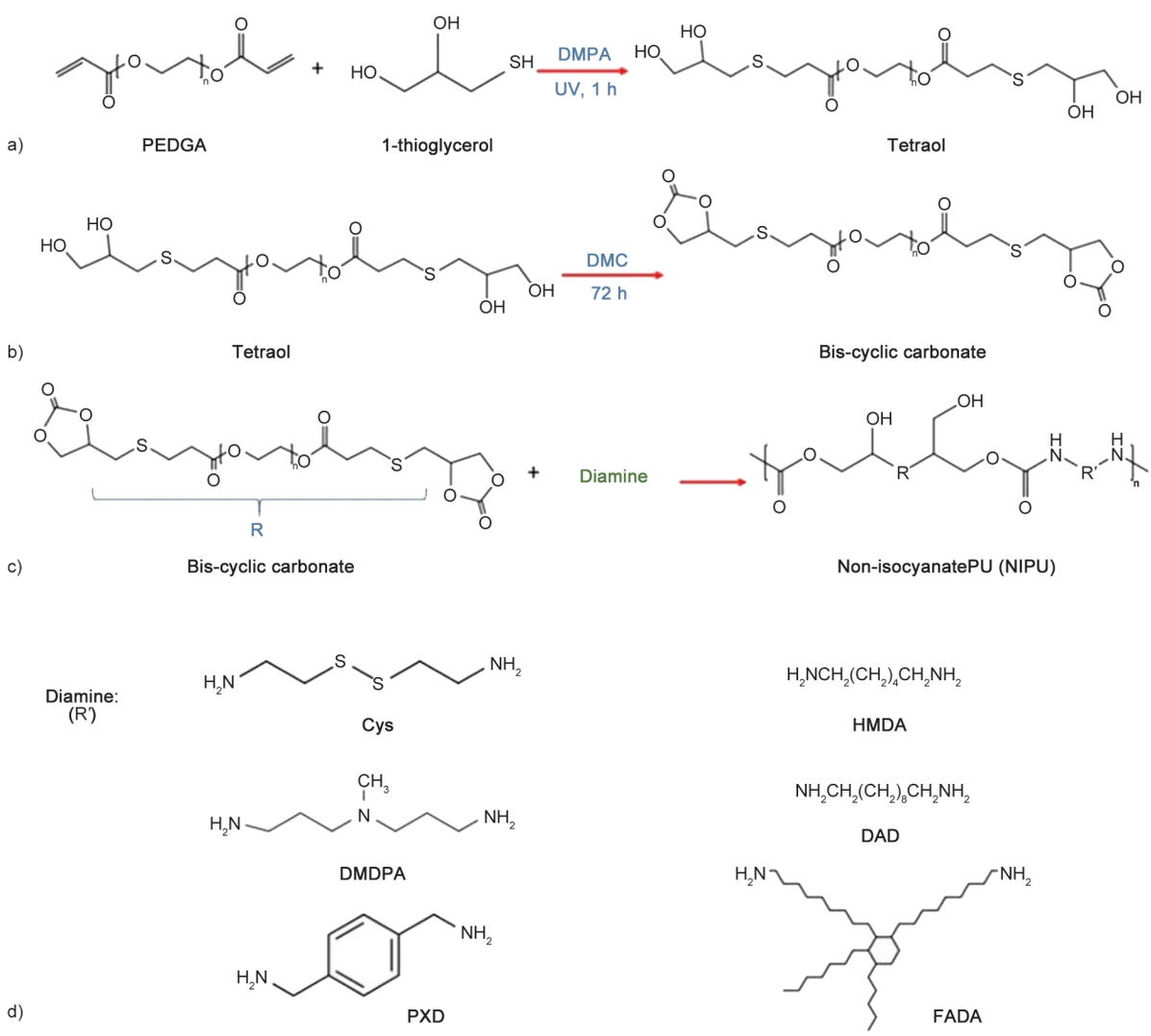

Figure 1. The synthesis procedure of (a) tetraol, (b) bis-cyclic carbonate, and (c) NIPUs. d) the molecular structure of six different diamines.

and six different diamines. The reaction is presented in Figure 1c. Furthermore, the chemical structure of the employed diamines is provided in Figure 1d. In the current study, for all NIPUs, the molar ratio of bis-cyclic carbonate to diamine was 1:1. For instance, a solution of 10 g bis-cyclic carbonate (19.2 mmol) and Cys (19.2 mmol) in 38.5 ml of DMSO (1 mol·l^{-1}) was prepared in an inert atmosphere and heated for 24 h at 100 °C. TEA was used to activate Cys. The molar ratio of TEA:Cys was 2:1. The product was precipitated in acetone, washed twice, and dried in a vacuum oven.

The NIPU films were prepared using a solution casting method. Thus, an appropriate amount of NIPUs was diluted in a minor amount of DMF and stirred for about 2 h to prepare a homogeneous solution; then, the obtained clear solution was cast in a silicon mold and dried in an oven for 24 h at 80 °C, vacuum dried for 24 h, and peeled off completely.

2.5. Characterizations

Fourier transform infrared spectroscopy (FTIR) analysis was performed in a range of 500 cm^{-1} to 4000 cm^{-1} using a PerkinElmer FT-IR with an ATR spectrometer at a resolution and a scanning number of 4 cm^{-1} and 16, respectively.

Proton nuclear magnetic resonance (^{1}H-NMR) analysis was performed using a Bruker AVANCE-III 400 MHz spectrometer, operating with sample solutions of DMSO-d6 containing TMS as the internal standard and with 32 scans at room temperature. Chemical shifts were given in the δ scale in parts per million [ppm].

The dispersity index (DI) and molecular weight (M_w) of the synthesized polymers were measured with gel permeation chromatography (GPC) using an Agilent 1100 series device equipped with one Agilent 5 µm bed column. DMSO was used as a solvent and applied at a 1.0 ml·min^{-1} flow rate. The sample concentration was approximately 1 mg·ml^{-1}. Narrow molar mass distribution pullulan standards were used to calibrate the columns.

The crystallinity of the NIPU films was investigated using PANalytical X Pert Powder XRD (alpha-1) with Cu-K_α radiation (λ = 1.54 Å) at 45 kV and 40 mA. Furthermore, the crystallization behavior of the NIPU films was studied using an MT-DSC Q2000 analyzer equipped with an inter-cooler. The sample was heated from –60 to 200 °C with a rate of 10 °C·min^{-1} in a nitrogen atmosphere.

The thermal stability and degradation of the NIPU films were investigated by thermogravimetric analysis (TGA) using a TA instruments model Q500 in a nitrogen atmosphere in a temperature range from 30 to 600 °C under a heating rate of 10 °C·min^{-1}.

The mechanical properties of the NIPU films were evaluated using tensile analysis performed in an Instron 4204 universal tensile testing machine. The strip-shaped film with the dimensions of L = 20 mm, W = 5 mm, and T = 0.2 mm was stretched under a load and tensile rate of 2 kN and 2 mm·min^{-1}, respectively. The measurement was performed at 25 °C, with a relative humidity of 50%. All samples were conditioned at 25 °C and 50% relative humidity for 48 h prior to the test. The measurement was repeated three times, and the mean value ± error was reported.

The surface wettability of the film was investigated by monitoring the contact angle of a 5 µl water droplet on a Theta Flex optical tensiometer. The contact angle was measured immediately and 60 s after deposition. The surface of the film was cleaned with ethanol before measurement. Each measurement was repeated three times.

3. Results and discussion

3.1. Synthesis of NIPUs

In this study, sulfur-substituted bis-cyclic carbonates were initiated through a thiol-ene coupling of thioglycerol with PEGDA, followed by transcarbonation of the resulting diols using DMC. After that, aminolysis of the bis-cyclic carbonate was performed using six different diamines to synthesize NIPUs. In the first step, tetraol was synthesized through the thiol-ene click (TEC) reaction of PEGDA and 1-thioglycerol (Figure 1a). The TEC reaction was initiated under UV radiation (λ = 365 nm) at room temperature in the presence of DMPA as a photoinitiator. The TEC reaction is a widely used synthesis route to build carbon-sulfur (C–S) bonds. The TEC reaction, which requires simple reaction conditions, is a high-yield stereospecific reaction that generates either no by-products or safe by-products [31]. In the second step (Figure 1b), bis-cyclic carbonate was synthesized through the transcarbonation reaction of tetraol and an excess amount of DMC as the reactive solvent in the presence of K_2CO_3 as a catalyst. The transcarbonation reaction has been widely employed using linear carbonate to create cyclic carbonate moieties [20, 32]. This reaction has been achieved

using several heterogeneous and homogeneous acids and basic catalysts. However, it is reported that using K_2CO_3 as the basic homogeneous catalyst can lead to higher conversion and yields close to 100% [33]. As provided in Figure 1c, as the final step, NIPUs were synthesized *via* ring-opening aminolysis of the bis-cyclic carbonate with diamines as the most promising approach to developing non-isocyanate polyurethane [34]. According to the literature, the optimized bis-cyclic carbonate to diamine ratio was adjusted to 1:1 for the polyaddition reaction to getting the best NIPU performance [35]. In addition, no catalyst was used for this reaction because the reaction between diamines and five and six-membered cyclic carbonates can occur without any catalyst [36, 37]. Here, various types of diamines were used for aminolysis of the bis-cyclic carbonate to synthesize NIPUs with different functionalities and properties.

3.2. The chemical structure analysis

The chemical structure and functional groups of all synthesized products were investigated using the FTIR and ^{1}H-NMR techniques. The FTIR spectra of PEGDA as a reference, synthesized tetraol, and bis-cyclic carbonate are presented in Figure 2a. Furthermore, the FTIR spectra of all the synthesized NIPUs are shown in Figure 2b. In line with the literature, the FTIR spectrum of PEGDA showed a peak at 2680 cm^{-1} assigned to vibration of the –CH_2 group, and a series of bands at 1720, 1255, and 864 cm^{-1} originated from the C=O and C–O stretching and C=C bending, respectively [38]. The spectrum of tetraol revealed a broad peak at 3400 cm^{-1} attributed to the O–H groups, which could not be seen in the spectrum of PEGDA, indicating the grafting of hydroxyl groups through TEC reaction with thioglycerol. Likewise, after the transcarbonation reaction, a new signal was detected in the FTIR spectrum of bis-cyclic carbonate at 1780 cm^{-1}, which was attributed to the C=O vibration of the cyclic carbonate. The presence of this peak can prove the successful forming of the carbonate ring through the reaction between tetraol and dimethyl carbonate [39]. Significant differences could be seen in the spectra of bis-cyclic NIPUs compared to bis-cyclic carbonate. For instance, the peak at 1780 cm^{-1} allocated to the carbonyl group of cyclic carbonate disappeared, indicating that the cyclic carbonate groups were entirely reacted with diamines *via* the ring-opening reaction [14, 40]. Furthermore, new signals appeared at 3300 and 1700 cm^{-1}, assigning to the O–H/N–H vibrations and the C=O vibrations of the urethane bonds, respectively [41]. Moreover, two sharp peaks could be detected at 2930 and 2850 cm^{-1}, corresponding to the asymmetric and symmetric methylene groups in the aliphatic chain of diamines [42]. It i's noteworthy that hydrogen bonds induce a distinctive shift in the vibrational frequencies of O–H or N–H stretching modes when compared to their non-bonded counterparts. Specifically, the stretching frequencies of O–H or N–H bonds engaged in hydrogen bonding typically manifest as lower frequencies, resulting in a characteristic red shift. Additionally, hydrogen bonding can also contribute to peak broadening within the O–H or N–H stretching region, and it is's worth noting that the extent of peak broadening correlates with the strength of the hydrogen bonding interactions. Consequently, from our analysis, it can

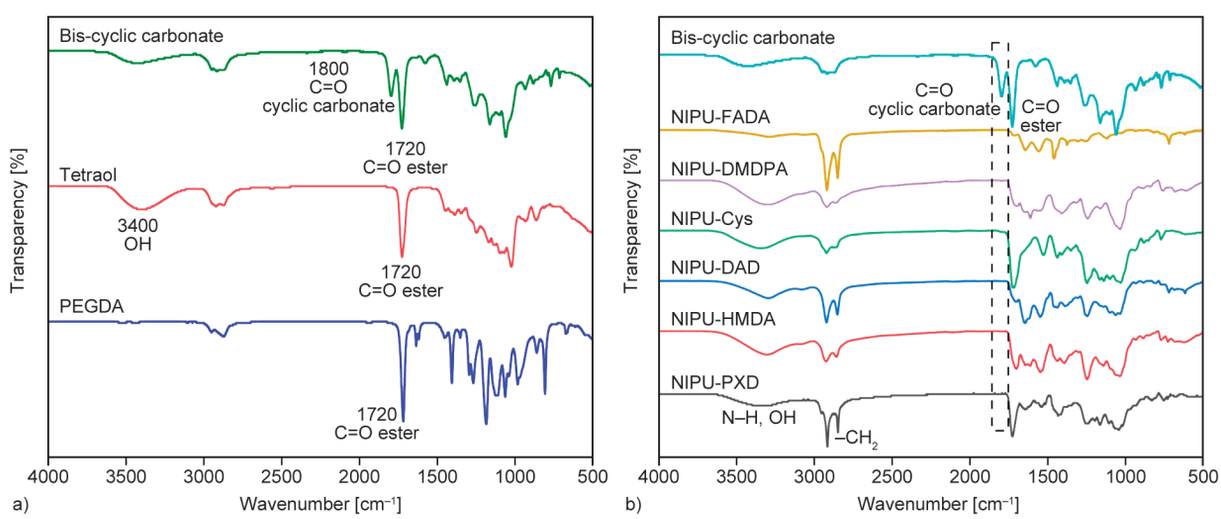

Figure 2. FTIR spectra of a) PEGDA, tetraol, and bis-cyclic carbonate and b) the synthesized NIPUs.

be assumed that hydrogen bonding played a more prominent role in the NIPU-PXD polymer as compared to other synthesized NIPUs.

^{1}H-NMR spectra were used to further study the molecular structure of the synthesized tetraol, bis-cyclic carbonate, and the synthesized NIPUs. The spectra of PEGDA as a reference, as well as tetraol and bis-cyclic carbonate, are presented in Figure 3. The PEGDA signals were assigned according to the literature. Namely, the peak in the range of 3 to 4 belonged to the PEGDA skeleton (–CH_2–), the signal between 4 to 4.5 was assigned to –CH_2O–CO–, and the peaks placed in the range of 5.5 to 6.5 were attributed to double bonds of PEGDA [43]. Some of these peaks repeated in the spectrum of tetraol; however, the disappearance of signals related to the double bonds of PEGDA at 5.5 to 6.5 ppm confirmed the consumption of double bonds during the TEC reaction of PEGDA and 1-thioglycerol [44]. Moreover, the appearance of the peak attributed to the nearby protons of the adjacent diol at 3.2 and 3.7 ppm could be considered as another proof of the successful synthesis of tetraol (marked as **a′**, **b′**, and **c′** in Figure 3b). Likewise, the synthesis of bis-cyclic carbonated through the transcarbonation reaction with DMC was confirmed by ^{1}H-NMR with the appearance of triplets around 4.1 to 4.5 ppm and a multiplet at 4.9 ppm (Figure 3c) [36, 40, 45].

The synthesis of NIPUs from bis-cyclic carbonate and six different diamines was also verified by

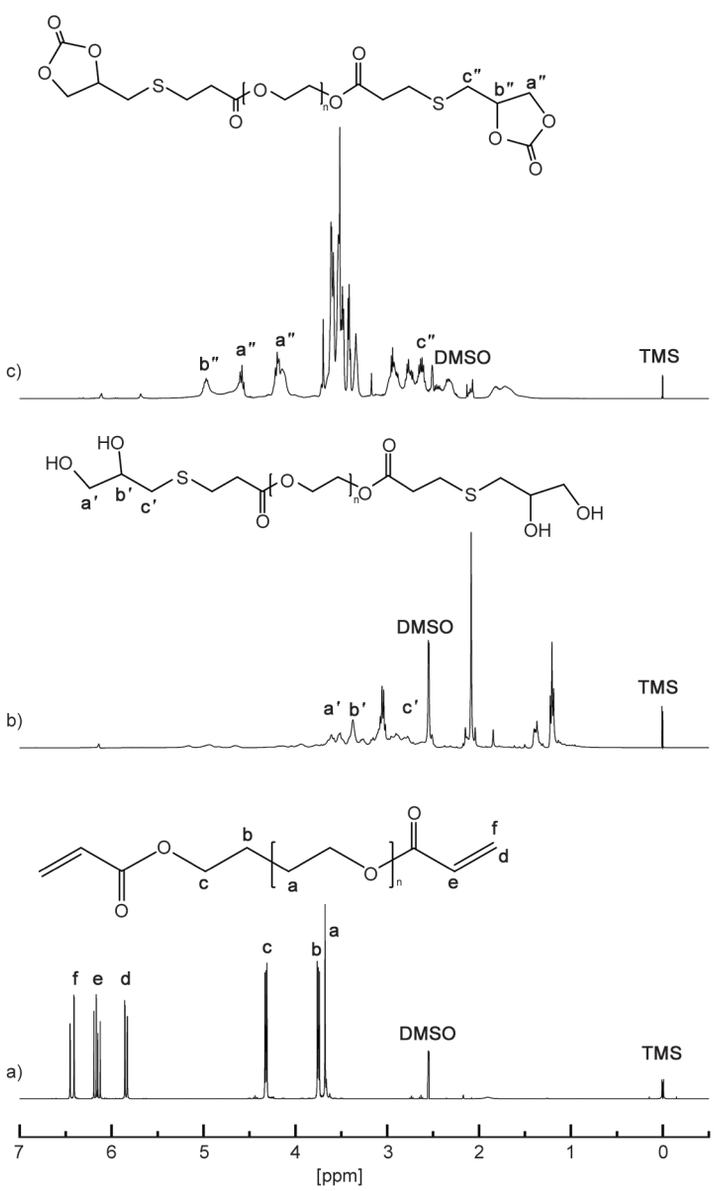

Figure 3. ^{1}H-NMR spectra of a) PEGDA, b) tetraol, and c) bis-cyclic carbonate in DMSO-d_6.

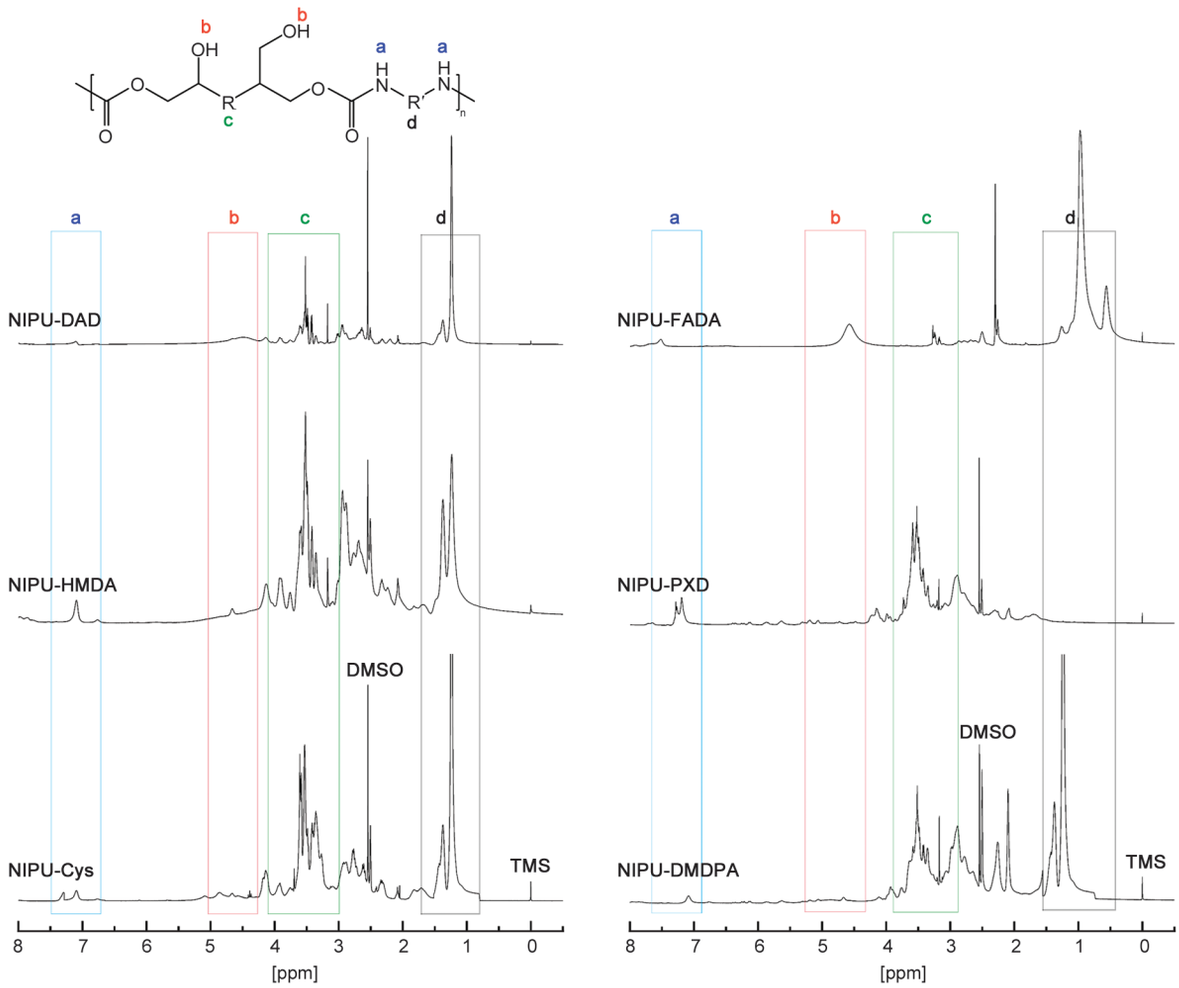

Figure 4. ^{1}H-NMR spectra of synthesized NIPUs in DMSO-d_6.

^{1}H-NMR, as illustrated in Figure 4. For instance, the vanishing of the cyclic-carbonate signals at 4.2 ppm and 4.6 ppm confirmed the conversion of carbonated groups. Furthermore, the successful synthesis of NIPUs was indicated by the new peaks detected at 6.9 to 7.5 ppm (marked as **a** in Figure 4), being associated with the urethane groups. Besides, small peaks at around 4.4 to 4.9 ppm (marked as **b** in Figure 4) confirmed the formation of the hydroxyl groups after the polyaddition of bis-cyclic carbonate and diamines. In addition, the signals that happened between 3 to 4 ppm (marked as **c** in Figure 4) were attributed to the protons in the alpha position to hydroxyl groups. Likewise, the signals that appeared between 0.5 to 1.5 ppm (marked as **d** in Figure 4) were ascribed to protons in alpha to nitrogen [34, 46].

3.3. Gel permeation chromatography (GPC)

GPC was done to determine molecular weight distribution (*e.g.*, dispersity index, DI) and relative molecular weight (*e.g.*, number average molecular weight, M_n and weight average molecular weight, M_w) of the synthesized NIPUs dissolved in DMSO. The results are provided in Table 1. The molecular weight of the synthesized NIPUs in this work was comparable to other NIPUs reported by other researchers who used different carbonates (*e.g.*, 5- and 6-membered ring carbonate) and diamine compounds [47, 48]. This suggests that the polymerization conditions, including time, temperature, and mechanical agitation during the ring-opening reaction, enhanced chain growth and reduced the probability of chain scission (degradation). Furthermore,

Table 1. M_n, M_w, and DI of the synthesized NIPUs.

Polymers	M_n [g·mol^{-1}]	M_w [g·mol^{-1}]	DI
NIPU-Cys	7 800	8 000	1.02
NIPU-HMDA	25 800	26 160	1.01
NIPU-DAD	43 100	61 600	1.43
NIPU-DMDPA	44 330	51 140	1.15
NIPU-FADA	42 300	48 500	1.14
NIPU-PXD	55 600	71 700	1.28

for all products, the value of M_w was higher than that of M_n, which is compatible with the theory of molecular weights for polymers [49]. However, the type of diamines significantly impacted the molecular weight of NIPUs due to their different reactivity toward the carbonate group. Namely, NIPU-PXD had the highest molecular weight than other NIPUs, and on the other hand, the lowest molecular weight was for NIPU-Cys. The reason for this phenomenon could be that the amine groups in cysteamine are sterically hindered by sulfur in the backbone of cysteamine, leading to a limited reactivity between the amine group and cyclic carbonate group, thus probably requiring harsh reaction conditions [50]. More importantly, all the polymers presented narrow molecular weight distribution, with the DI values being less than 1.5, indicating uniform molecular size. Furthermore, there was no remarkable peak in the GPC curves, confirming that the polymerization proceeded more efficiently without any side reactions during polymerization [24, 51], which were also proved by the FTIR and ^{1}H-NMR spectrums. The narrow molecular weight distribution, which is favorable to the synthesis of NIPU films, could also suggest better NIPU performances [35].

3.4. Crystallization study of the synthesized NIPUs

XRD was applied to study the morphology and crystallinity of the synthesized NIPUs. The XRD patterns are presented in Figure 5. All polymers provided a broad diffuse peak at 2θ = 20° followed by one broader peak with very low intensity at 2θ = 43°. None of the NIPUs presented a sharp diffraction peak, indicating that they were amorphous and there were no crystalline structures in these polymers [52]. Ghasemlou *et al*. [53] observed sharp diffraction peaks at 2θ angles of 18.5°, 19.2°, 20.6°, 21.7°, and 22.9° for the NIPUs synthesized by the reaction between ethylene carbonate and different diamines, concluding very high degree of crystallinity. The most amorphous structure of the synthesized NIPUs in our study could be due to strong hydrogen bonding between hydroxyl groups of NIPUs, which reduced the mobility of the molecular chain of PUs and restricted their crystallization. Although all PUs possessed an amorphous structure, the intensity of the amorphous at 2θ = 20° was significantly different due to the diamine type. The lowest peak intensity was observed in NIPU-PXD and NIPU-DMDPA, indicating stronger inter and intramolecular interactions, *e.g.*, hydrogen bonding [54], compared to other NIPUs.

DSC analysis was carried out to further investigate the crystalline structure of the developed NIPUs. The thermograms are depicted in Figure 5b. Based on the DSC results, the amorphous structure of the synthesized NIPUs could be confirmed by not seeing any phase change peaks, such as melting or crystallization peaks in the test temperature range, which is in line with XRD results. Specifically, all samples presented a step in the region –20 to 20 °C, corresponding to the glass transition of the materials, where the amorphous polymer changed from a glassy state to a rubbery one. The glass transition temperature (T_g) values are summarized in Table 2, where all the NIPUs presented a single T_g that was below room temperature, indicating that all samples exhibited a

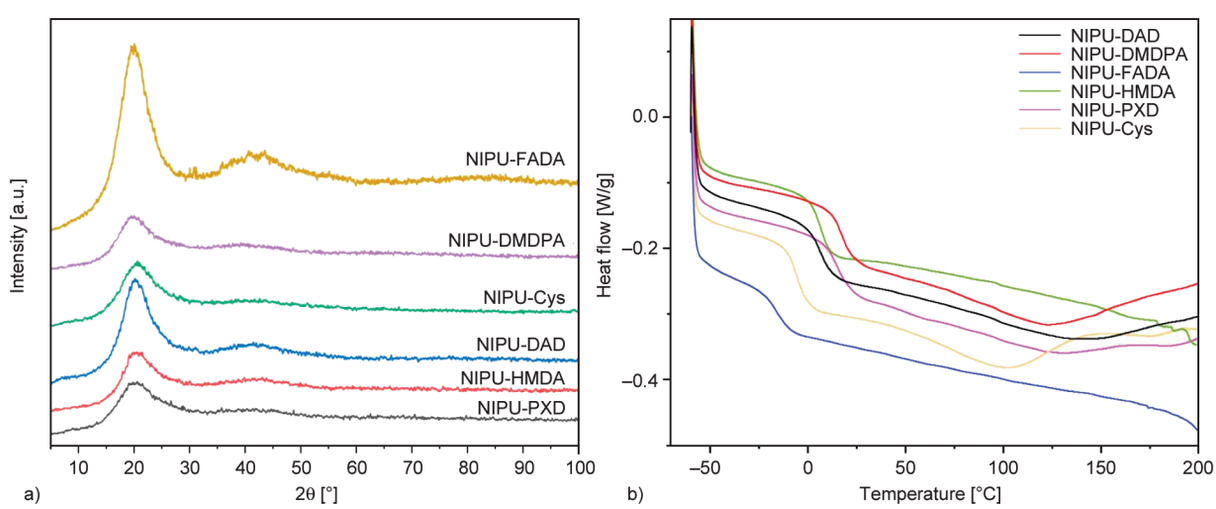

Figure 5. a) XRD patterns and b) DSC curves of the synthesized NIPUs.

rubbery state at ambient temperature. The T_g values were well-fitted with those reported for PUs by other researchers [55–57]. It is worth highlighting that two intensely overlapped components have been observed around the T_g of PUs, indicating a very weak internal structure due to heterogeneity caused by the disruption of the network [55, 58]. A single T_g for all NIPUs in the current confirmed no micro-phase separation or interrupted networks within the polymerization. In other words, the hard and soft segments were completely miscible. The highest T_g values were for NIPUs containing DMDPA and PXD diamine, indicating decelerated chain mobility, most likely due to rigid aromatic rings and nitrogen-containing functional groups in the polymer backbone as well as strong hydrogen bonding between the polymer chains, restricting the chains' mobility [59]. Likewise, the NIPU-FADA demonstrated the lowest T_g, which could be attributed to long flexible arms that resulted in a significant decrease in the regularity and symmetry of the chain segments as well as a reduction in the density of hydrogen bonding between polymer chains [60].

3.5. Thermal stability

The thermal stability of the synthesized NIPUs was investigated using thermogravimetric analysis (TGA) to study the correlation between diamines, structure, and polymer thermal properties. Figure 6 presents the weight loss (TGA) and derivative weight loss (DTG) of the polymers in the temperature ranging from 30 to 600 °C. Furthermore, the relevant data, including the degradation onset temperature at 5 and 10% weight loss ($T_{d5\%}$, $T_{d10\%}$), maximum weight loss (T_{max1}, T_{max2}), and residual mass yield (RM%), are summarized in Table 2. In an inert atmosphere, all studied polymers exhibit a two-step degradation pattern corresponding to the standard thermal decomposition of conventional PUs and other NIPUs [10], concluding that all kinds of developed NIPUs in this study followed the same thermal degradation pattern. The first decomposition step, which was the largest mass loss, occurred at temperatures ranging from 220–290 °C, assigned to the decomposition of urethane bonds. Urethane bonds are the most thermally labile fragments in NIPU chains, and their decomposition, which results from the breaking of the –C–N bond, forms ammonia, carbon dioxide, and carbon oxide. This step overlapped with the second decomposition stage, which happened from 400 to 460 °C, attributed to the C–C bond cleavage and rapid decomposition of ether bonds and aliphatic hydrocarbon chains of diamine constituents [13, 14, 61]. With careful looking at the TGA/DTG thermograms, significant differences in the thermal decomposition of the synthesized NIPUs with different diamines can be seen. In other words, the mechanism of NIPU degradation was governed by the kind of diamine used within the polymer synthesis process. Namely, the highest T_{max1}, belonging to urethane

Table 2. TGA and DSC data of NIPUs.

Polymers	$T_{d5\%}$ [°C]	$T_{d10\%}$ [°C]	T_{max1} [°C]	T_{max2} [°C]	RM%	T_g [°C]
NIPU-Cys	225	241	283	404	11.06	–5.32
NIPU-HMDA	220	247	265	436	5.27	5.96
NIPU-DAD	236	258	276	452	3.12	5.95
NIPU-DMDPA	222	240	257	425	9.02	17.21
NIPU-FADA	213	227	221	456	4.00	–15.45
NIPU-PXD	237	262	288	406	15.03	15.40

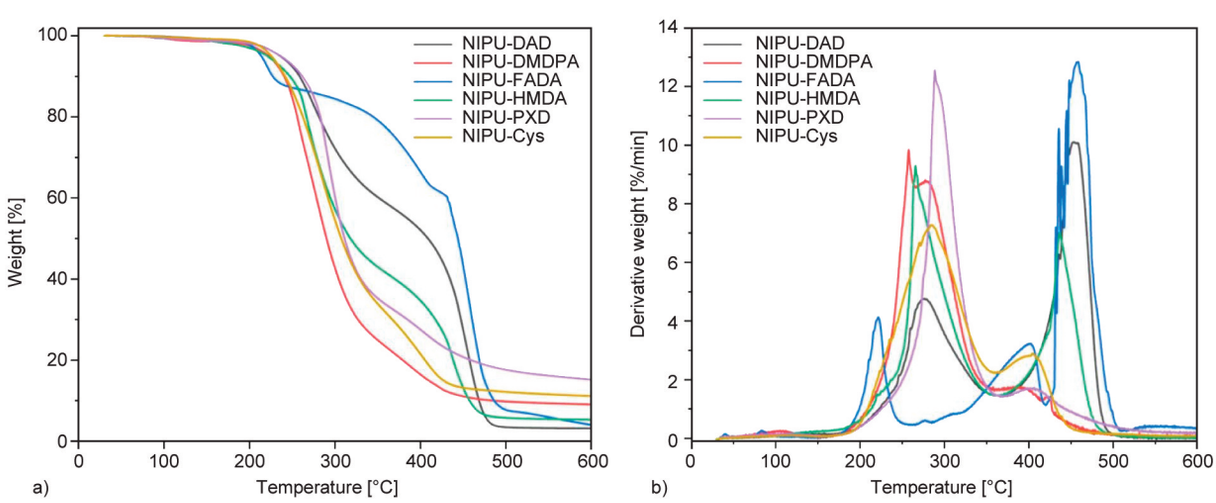

Figure 6. a) TGA and b) DTG thermograms of NIPUs in the temperature range of 30 to 600 °C under a nitrogen atmosphere.

bond decomposition, was seen in the NIPU-PXD, suggesting the lower urethane content in this formulation [8]. This sample also presented the highest $T_{d5\%}$ and $T_{d10\%}$, indicating its higher thermal stability compared to other polymers. This could be due to having cyclic aromatic structures, which leads to better preserving the overall structure of NIPU upon heating. The higher thermal stability of this sample could also be due to its high inter and intramolecular interactions, *e.g.*, hydrogen bonding, shielding the hydroxyl groups to a certain extent, hence preventing the decomposition of their main backbones [62]. It has been reported that the aromatic parts of amine compounds could also make relatively high char yield at 600 °C [9, 63], as in our work, the NIPU-PXD had the highest *RM*% compared to other NIPUs. On the other hand, the NIPU-FADA, formed from aliphatic pendant chains, was more prone to decompose at lower temperatures than the other polymers, most likely due to the long, flexible hydrocarbon chains in its structure.

3.6. Mechanical properties

A tensile film test with a stretching rate of 2 mm·min^{-1} was performed to investigate the mechanical properties of NIPUs. The typical stress-strain curves are presented in Figure 7a. In addition, the relevant data are presented in Table 3. It was found that the mechanical properties of the synthesized NIPUs were governed by the diamine types. Namely, NIPU-FADA presented the lowest stiffness, where Young's modulus was 14±0.9 MPa. However, it had the highest tensile strain at break of 47±3%. This behavior could be explained by the presence of FADA with a four-branched structure, providing a relatively soft and flexible property for the synthesized NIPU. It has also been reported by other researchers that the incorporation of the FADA could enhance the tensile strain at break by increasing the amount of soft segment [40]. On the other hand, NIPU-DMDPA exhibited the greatest value for Young's modulus and the lowest value for tensile strain at break, which was compatible with the structural properties of diamine as the soft segment part. DMDPA contains a nitrogen atom in the structure of diamine, which increases its rigidity due to its trigonal pyramidal configuration and the highest density of hydrogen bonds between polymer chains, providing more physical crosslinking [12].

3.7. Surface wettability

A water contact angle measurement was carried out to monitor the surface wettability of the developed NIPUs as potential coating materials. Figure 7b shows the initial water contact angles of 1 and 60 s after the drop contact with the material surface. Except for NIPU-Cys, the rest of the polymers provided

Table 3. Mechanical properties of synthesized NIPUs (n = 5, average ± SD).

Polymers	Young's modulus [MPa]	Tensile stress [MPa]	Tensile strain at break [%]
NIPU-FADA	14±0.9	1.43±0.05	47±3
NIPU-HMDA	30±1.0	2.67±0.14	31±2
NIPU-PXD	78 ±1.7	10.98±0.71	26±2
NIPU-DAD	26±3.0	4.21±0.23	25±3
NIPU-Cys	17±1.8	2.85±0.19	20±2
NIPU-DMDPA	106±9.0	12.26±0.91	15±1

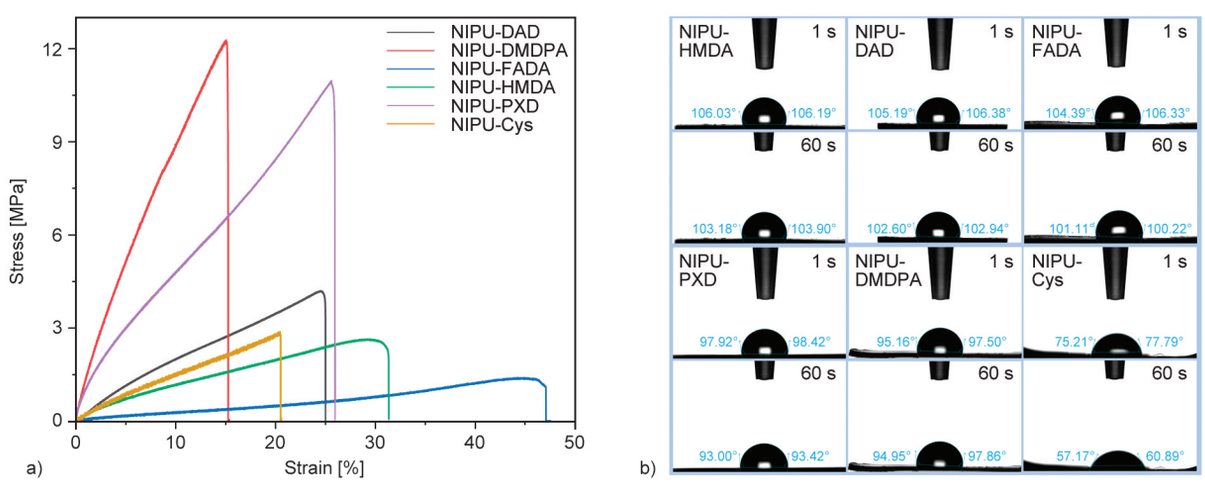

Figure 7. a) Stress-strain curves and b) the water contact angle 1 and 60 s after the droplet was placed on the surface of the synthesized NIPUs.

a water contact angle higher than 90°, indicating a hydrophobic surface enriched by nonpolar regions [64]. The relatively lower contact angle in the NIPU-Cys (~75°) could be attributed to the more hydrophilic nature of cysteamine than the rest of the diamines. The contact angle was further reduced to ~60° after 60 s, indicating the tension of the surface to absorb water. Mosikatsi *et al*. [65] also reported a contact angle of 70° for polyethersulfone hyperbranched polyethyleneimine cysteamine composite. The water contact angle for the rest of the NIPUs was located at 95–107°, similar to the results of other researchers who have developed PUs for coating applications. Furthermore, the differences between the contact angles 1 and 60 s after droplet deposition were negligible, indicating that the film surfaces exhibited good homogeneity [66]. It should be highlighted that a significantly higher water contact angle has been reported for PU-based coatings; however, in most of those, an additive was used to improve the surface hydrophobicity [67, 68].

4. Conclusions

A new semi-bio-based bis-cyclic carbonate was designed and developed through the transcarbonation reaction of synthesized PEG containing tetraol using K_2CO_3 as a catalyst. Then, several NIPUs were introduced by the polyaddition of bis-cyclic carbonate and six different diamines. The spectral and chemical properties of the polymers and their physical properties were studied to investigate the effect of using various diamines on the final properties of the NIPUs. In this study, linear and branched NIPUs were synthesized with T_g values ranging from –15.45 to 17.21 °C, of which the low T_g NIPUs are suitable for coating applications. According to the TGA results, all synthesized NIPUs showed acceptable thermal stability with the T_d in the 213–237 °C range. Of all the NIPUs, the NIPU-PXD showed the highest residual content at 600 °C, as it contained aromatic moiety, which provided the highest char content compared with aliphatic chains; thus, this property might be interesting for flame-retardant applications. The mechanical test results also revealed that the NIPU prepared by fatty acid-based diamine (NIPU-FADA) demonstrated a lower Young's modulus and higher tensile strain at break because of its four-branched structure and greater flexibility. On the other hand, NIPU-DMDPA showed a higher Young's modulus and lower tensile strain at break, as it contains a nitrogen atom in its structure and a trigonal pyramidal configuration with the highest density of hydrogen bonds between polymer chains, thereby increasing its rigidity. Furthermore, the water contact angle results proved significant surface hydrophobicity for most of the developed NIPUs, making them interesting for coating applications.

Acknowledgements

The authors would like to thank the Magnus Ehrnrooth Foundation, Finnish Cultural Foundation, and Academy of Finland No. 307485 (3D-Biomat) for providing funding for this project. This work made use of the Bioeconomy infrastructure at Aalto University.

References

[1] Cornille A., Auvergne R., Figovsky O., Boutevin B., Caillol S.: A perspective approach to sustainable routes for non-isocyanate polyurethanes. European Polymer Journal, **87**, 535–552 (2017). https://doi.org/10.1016/j.eurpolymj.2016.11.027

[2] Stachak P., Łukaszewska I., Hebda E., Pielichowski K.: Recent advances in fabrication of non-isocyanate polyurethane-based composite materials. Materials, **14**, 3497 (2021). https://doi.org/10.3390/ma14133497

[3] Farzan A., Borandeh S., Seppälä J.: Conductive polyurethane/PEGylated graphene oxide composite for 3D-printed nerve guidance conduits. European Polymer Journal, **167**, 111068 (2022). https://doi.org/10.1016/j.eurpolymj.2022.111068

[4] Engels H-W., Pirkl H-G., Albers R., Albach R. W., Krause J., Hoffmann A., Casselmann H., Dormish J.: Polyurethanes: Versatile materials and sustainable problem solvers for today's challenges. Angewandte Chemie: International Edition, **52**, 9422–9441 (2013). https://doi.org/10.1002/anie.201302766

[5] John J., Bhattacharya M., Turner R. B.: Characterization of polyurethane foams from soybean oil. Journal of Applied Polymer Science, **86**, 3097–3107 (2002). https://doi.org/10.1002/app.11322

[6] Krone C. A., Ely J. T. A., Klingner T., Rando R. J.: Isocyanates in flexible polyurethane foams. Bulletin of Environmental Contamination and Toxicology, **70**, 328–335 (2003). https://doi.org/10.1007/s00128-002-0195-2

[7] Allport D. C., Gilbert D. S., Outterside S. M.: MDI and TDI: Safety, health and the environment, A source book and practical guide. Wiley, Manchester (2003).

[8] Ling Z., Zhang C., Zhou Q.: Synthesis and characterization of 1 K waterborne non-isocyanate polyurethane epoxy hybrid coating. Progress in Organic Coatings, **169**, 106915 (2022). https://doi.org/10.1016/j.porgcoat.2022.106915

[9] Błażek K., Kasprzyk P., Datta J.: Diamine derivatives of dimerized fatty acids and bio-based polyether polyol as sustainable platforms for the synthesis of non-isocyanate polyurethanes. Polymer, **205**, 122768 (2020). https://doi.org/10.1016/j.polymer.2020.122768

[10] Bukowczan A., Stachak P., Łukaszewska I., Majka T. M., Hebda E., Pielichowski K.: Pyrolysis and thermal degradation studies of non-isocyanate polyurethanes modified by polyhedral oligomeric silsesquioxanes. Thermochimica Acta, **723**, 179484 (2023). https://doi.org/10.1016/j.tca.2023.179484

[11] Rokicki G., Parzuchowski P. G., Mazurek M.: Non-isocyanate polyurethanes: Synthesis, properties, and applications. Polymers for Advanced Technologies, **26**, 707–761 (2015). https://doi.org/10.1002/pat.3522

[12] Maisonneuve L., Lamarzelle O., Rix E., Grau E., Cramail H.: Isocyanate-free routes to polyurethanes and poly (hydroxy urethane)s. Chemical Reviews, **115**, 12407–12439 (2015). https://doi.org/10.1021/acs.chemrev.5b00355

[13] Singh P., Kaur R.: One pot synthesis of bio-based porous isocyanate-free polyurethane materials. Materials Letters, **331**, 133433 (2023). https://doi.org/10.1016/j.matlet.2022.133433

[14] Zhang T., Xue B., Yan Q., Yuan Y., Tan J., Guan Y., Wen J., Li X., Zhao W.: New kinds of lignin/non-isocyanate polyurethane hybrid polymers: Facile synthesis, smart properties and adhesive applications. Industrial Crops and Products, **199**, 116706 (2023). https://doi.org/10.1016/j.indcrop.2023.116706

[15] Clark J. H., Farmer T. J., Ingram I. D. V., Lie Y., North M.: Renewable self-blowing non-isocyanate polyurethane foams from lysine and sorbitol. European Journal of Organic Chemistry, **2018**, 4265–4271 (2018). https://doi.org/10.1002/ejoc.201800665

[16] Singh P., Kaur R.: Sustainable xylose-based non-isocyanate polyurethane foams with remarkable fire-retardant properties. Journal of Polymers and the Environment, **31**, 743–753 (2023). https://doi.org/10.1007/s10924-022-02638-4

[17] Malik M., Kaur R.: Synthesis of NIPU by the carbonation of canola oil using highly efficient 5,10,15-tris (pentafluorophenyl)corrolato-manganese(III) complex as novel catalyst. Polymers for Advanced Technologies, **29**, 1078–1085 (2018). https://doi.org/10.1002/pat.4219

[18] Benyahya S., Desroches M., Auvergne R., Carlotti S., Caillol S., Boutevin B.: Synthesis of glycerin carbonate-based intermediates using thiol–ene chemistry and isocyanate free polyhydroxyurethanes therefrom. Polymer Chemistry, **2**, 2661–2667 (2011). https://doi.org/10.1039/C1PY00289A

[19] Schäffner B., Schäffner F., Verevkin S. P., Börner A.: Organic carbonates as solvents in synthesis and catalysis. Chemical Reviews, **110**, 4554–4581 (2010). https://doi.org/10.1021/cr900393d

[20] Pescarmona P. P.: Cyclic carbonates synthesised from CO_2: Applications, challenges and recent research trends. Current Opinion in Green and Sustainable Chemistry, **29**, 100457 (2021). https://doi.org/10.1016/j.cogsc.2021.100457

[21] Marciniak A. A., Lamb K. J., Ozorio L. P., Mota C. J. A., North M.: Heterogeneous catalysts for cyclic carbonate synthesis from carbon dioxide and epoxides. Current Opinion in Green and Sustainable Chemistry, **26**, 100365 (2020). https://doi.org/10.1016/j.cogsc.2020.100365

[22] Xu B-H., Wang J-Q., Sun J., Huang Y., Zhang J-P., Zhang X-P., Zhang S-J.: Fixation of CO_2 into cyclic carbonates catalyzed by ionic liquids: A multi-scale approach. Green Chemistry, **17**, 108–122 (2015). https://doi.org/10.1039/C4GC01754D

[23] Carré C., Zoccheddu H., Delalande S., Pichon P., Avérous L.: Synthesis and characterization of advanced biobased thermoplastic nonisocyanate polyurethanes, with controlled aromatic-aliphatic architectures. European Polymer Journal, **84**, 759–769 (2016). https://doi.org/10.1016/j.eurpolymj.2016.05.030

[24] Yang Y., Cao H., Wang Y., Zhao J., Ren W., Wang B., Qin P., Chen F., Wang Y., Cai D.: Non-isocyanate polyurethane from sweet potato residual and the application in food preservation. Industrial Crops and Products, **186**, 115224 (2022). https://doi.org/10.1016/j.indcrop.2022.115224

[25] Tomazett V. K., Chacon G., Marin G., Castegnaro M. V., das Chagas R. P., Lião L. M., Dupont J., Qadir M. I.: Ionic liquid confined spaces controlled catalytic CO_2 cycloaddition of epoxides in BMIm.$ZnCl_3$ and its supported ionic liquid phases. Journal of CO_2 Utilization, **69**, 102400 (2023). https://doi.org/10.1016/j.jcou.2023.102400

[26] Mimini V., Amer H., Hettegger H., Bacher M., Gebauer I., Bischof R., Fackler K., Potthast A., Rosenau T.: Lignosulfonate-based polyurethane materials *via* cyclic carbonates: Preparation and characterization. Holzforschung, **74**, 203–211 (2020). https://doi.org/10.1515/hf-2018-0298

[27] Patel P. N., Smith C. K., Patrick C. W.: Rheological and recovery properties of poly(ethylene glycol) diacrylate hydrogels and human adipose tissue. Journal of Biomedical Materials Research Part A, **73**, 313–319 (2005). https://doi.org/10.1002/jbm.a.30291

[28] Beamish J. A., Zhu J., Kottke-Marchant K., Marchant R. E.: The effects of monoacrylated poly(ethylene glycol) on the properties of poly(ethylene glycol) diacrylate hydrogels used for tissue engineering. Journal of Biomedical Materials Research Part A, **92**, 441–450 (2010). https://doi.org/10.1002/jbm.a.32353

[29] Wu J., Wang C., Xiao Y., Mu C., Lin W.: Fabrication of water-resistance and durable antimicrobial adhesion polyurethane coating containing weakly amphiphilic poly(isobornyl acrylate) side chains. Progress in Organic Coatings, **147**, 105812 (2020). https://doi.org/10.1016/j.porgcoat.2020.105812

[30] Tork L., Rottmaier L., Höhne W.: Formulations and process for dressing leather and coating textiles. US5087646A, U.S. Patent, USA (1992).

[31] Sinha A. K., Equbal D.: Thiol–ene reaction: Synthetic aspects and mechanistic studies of an anti-markovnikov-selective hydrothiolation of olefins. Asian Journal of Organic Chemistry, **8**, 32–47 (2019). https://doi.org/10.1002/ajoc.201800639

[32] Mignani G., Debray J., Lemaire M., Raoul Y.: Method for producing polyglycerol (poly)carbonate. US9242956B2, U.S. Patent, USA (2016).

[33] Ochoa-Gómez J. R., Gómez-Jiménez-Aberasturi O., Maestro-Madurga B., Pesquera-Rodríguez A., Ramírez-López C., Lorenzo-Ibarreta L., Torrecilla-Soria J., Villarán-Velasco M. C.: Synthesis of glycerol carbonate from glycerol and dimethyl carbonate by transesterification: Catalyst screening and reaction optimization. Applied Catalysis A: General, **366**, 315–324 (2009). https://doi.org/10.1016/j.apcata.2009.07.020

[34] Pérez-Sena W. Y., Cai X., Kebir N., Vernières-Hassimi L., Serra C., Salmi T., Leveneur S.: Aminolysis of cyclic-carbonate vegetable oils as a non-isocyanate route for the synthesis of polyurethane: A kinetic and thermal study. Chemical Engineering Journal, **346**, 271–280 (2018). https://doi.org/10.1016/j.cej.2018.04.028

[35] Yang Y., Cao H., Liu R., Wang Y., Zhu M., Su C., Lv X., Zhao J., Qin P., Cai D.: Fabrication of ultraviolet resistant and anti-bacterial non-isocyanate polyurethanes using the oligomers from the reductive catalytic fractionated lignin oil. Industrial Crops and Products, **193**, 116213 (2023). https://doi.org/10.1016/j.indcrop.2022.116213

[36] Lamarzelle O., Hibert G., Lecommandoux S., Grau E., Cramail H.: A thioglycerol route to bio-based bis-cyclic carbonates: Poly(hydroxyurethane) preparation and post-functionalization. Polymer Chemistry, **8**, 3438–3447 (2017). https://doi.org/10.1039/C7PY00556C

[37] Pyo S-H., Persson P., Mollaahmad M. A., Sörensen K., Lundmark S., Hatti-Kaul R.: Cyclic carbonates as monomers for phosgene- and isocyanate-free polyurethanes and polycarbonates. Pure and Applied Chemistry, **84**, 637–661 (2012). https://doi.org/10.1351/PAC-CON-11-06-14

[38] Rani I., Warkar S. G., Kumar A.: Nano ZnO embedded poly(ethylene glycol) diacrylate cross-linked carboxy methyl tamarind kernel gum (CMTKG)/poly (sodium acrylate) composite hydrogels for oral delivery of ciprofloxacin drug and their antibacterial properties. Materials Today Communications, **35**, 105635 (2023). https://doi.org/10.1016/j.mtcomm.2023.105635

[39] Coste G., Berne D., Ladmiral V., Negrell C., Caillol S.: Non-isocyanate polyurethane foams based on six-membered cyclic carbonates. European Polymer Journal, **176**, 111392 (2022). https://doi.org/10.1016/j.eurpolymj.2022.111392

[40] Zhang C., Wang H., Zhou Q.: Waterborne isocyanate-free polyurethane epoxy hybrid coatings synthesized from sustainable fatty acid diamine. Green Chemistry, **22**, 1329–1337 (2020). https://doi.org/10.1039/C9GC03335A

[41] Błażek K., Beneš H., Walterová Z., Abbrent S., Eceiza A., Calvo-Correas T., Datta J.: Synthesis and structural characterization of bio-based bis(cyclic carbonate)s for the preparation of non-isocyanate polyurethanes. Polymer Chemistry, **12**, 1643–1652 (2021). https://doi.org/10.1039/D0PY01576H

[42] Baniasadi H., Lipponen S., Asplund M., Seppälä J.: High-concentration lignin biocomposites with low-melting point biopolyamide. Chemical Engineering Journal, **451**, 138564 (2023). https://doi.org/10.1016/j.cej.2022.138564

[43] Liu Q., Peña J., Xing J.: Rapid preparation of nanogels by photopolymerization at 532 nm. Colloids and Surfaces B: Biointerfaces, **206**, 111943 (2021). https://doi.org/10.1016/j.colsurfb.2021.111943

[44] Bao Y., He J., Li Y.: Facile and efficient synthesis of hyperbranched polyesters based on renewable castor oil. Polymer International, **62**, 1457–1464 (2013). https://doi.org/10.1002/pi.4440

[45] Schimpf V., Asmacher A., Fuchs A., Bruchmann B., Mülhaupt R.: Polyfunctional acrylic non-isocyanate hydroxyurethanes as photocurable thermosets for 3D printing. Macromolecules, **52**, 3288–3297 (2019). https://doi.org/10.1021/acs.macromol.9b00330

[46] van Velthoven J. L. J., Gootjes L., van Es D. S., Noordover B. A. J., Meuldijk J.: Poly(hydroxy urethane)s based on renewable diglycerol dicarbonate. European Polymer Journal, **70**, 125–135 (2015). https://doi.org/10.1016/j.eurpolymj.2015.07.011

[47] Kathalewar M., Sabnis A., D'Mello D.: Isocyanate free polyurethanes from new CNSL based bis-cyclic carbonate and its application in coatings. European Polymer Journal, **57**, 99–108 (2014). https://doi.org/10.1016/j.eurpolymj.2014.05.008

[48] Ngo D. M., Lee K., Ho L. N. T., Lee J., Jung H. M.: Direct conversion of waste polyesters to low molecular weight polyols for polyurethane production. Polymer Degradation and Stability, **205**, 110147 (2022). https://doi.org/10.1016/j.polymdegradstab.2022.110147

[49] Odian G.: Principles of polymerization. Wiley, New Jersey (2004).

[50] Meng X., Zhang S., Scheidemantle B., Wang Y-Y., Pu Y., Wyman C. E., Cai C. M., Ragauskas A. J.: Preparation and characterization of aminated *co*-solvent enhanced lignocellulosic fractionation lignin as a renewable building block for the synthesis of non-isocyanate polyurethanes. Industrial Crops and Products, **178**, 114579 (2022). https://doi.org/10.1016/j.indcrop.2022.114579

[51] Sánchez–Adsuar M. S., Papon E., Villenave J.: Influence of the prepolymerization on the properties of thermoplastic polyurethane elastomers. Part I. Prepolymer characterization. Journal of Applied Polymer Science, **76**, 1596–1601 (1999). https://doi.org/10.1002/(SICI)1097-4628(20000606)76:10<1596::AID-APP15>3.0.CO;2-U

[52] Wei Z., Liu Z., Fu X., Wang Y., Yuan A., Lei J.: Effect of crystalline structure on water resistance of waterborne polyurethane. European Polymer Journal, **157**, 110647 (2021). https://doi.org/10.1016/j.eurpolymj.2021.110647

[53] Ghasemlou M., Daver F., Ivanova E. P., Adhikari B.: Synthesis of green hybrid materials using starch and non-isocyanate polyurethanes. Carbohydrate Polymers, **229**, 115535 (2020). https://doi.org/10.1016/j.carbpol.2019.115535

[54] Amjed N., Bhatti I. A., Simon L., dal Castel C., Zia K. M., Zuber M., Hafiz I., Murtaza M. A.: Preparation and characterization of thermoplastic polyurethanes blended with chitosan and starch processed through extrusion. International Journal of Biological Macromolecules, **208**, 37–44 (2022). https://doi.org/10.1016/j.ijbiomac.2022.03.008

[55] Raftopoulos K. N., Łukaszewska I., Calduch C. B., Stachak P., Lalik S., Hebda E., Marzec M., Pielichowski K.: Hydration and glass transition of hybrid non-isocyanate polyurethanes with POSS inclusions. Polymer, **253**, 125010 (2022). https://doi.org/10.1016/j.polymer.2022.125010

[56] Lu R-Q., Concellón A., Wang P., Swager T. M., Hsieh A. J.: Supramolecular hierarchical polyurethane elastomers for thermal and mechanical property optimization. Polymer, **260**, 125363 (2022). https://doi.org/10.1016/j.polymer.2022.125363

[57] Zhao Y., Gong X., Liu Q.: Research on rheological properties and modification mechanism of waterborne polyurethane modified bitumen. Construction and Building Materials, **371**, 130775 (2023). https://doi.org/10.1016/j.conbuildmat.2023.130775

[58] Njuguna J., Muchiri P., Mwema F. M., Karuri N., Herzog M. T., Dimitrov K.: Determination of thermo-mechanical properties of recycled polyurethane from glycolysis polyol. International Journal of Manufacturing, Materials, and Mechanical Engineering (IJMMME), **11**, 75–87 (2021). https://doi.org/10.1016/j.sciaf.2021.e00755

[59] Bukowczan A., Raftopoulos K. N., Nizioł J., Pielichowski K.: Molecular mobility of liquid crystalline polyurethanes modified by polyhedral oligomeric silsesquioxanes. Polymer, **277**, 125981 (2023). https://doi.org/10.1016/j.polymer.2023.125981

[60] Xing W., Xi J., Qi L., Hai Z., Cai W., Zhang W., Wang B., Chen L., Hu Y.: Construction of a flame retardant polyurethane elastomer with degradability, high mechanical strength and shape memory. Composites Part A: Applied Science and Manufacturing, **169**, 107512 (2023). https://doi.org/10.1016/j.compositesa.2023.107512

[61] Farzan A., Borandeh S., Zanjanizadeh Ezazi N., Lipponen S., Santos H. A., Seppälä J.: 3D scaffolding of fast photocurable polyurethane for soft tissue engineering by stereolithography: Influence of materials and geometry on growth of fibroblast cells. European Polymer Journal, **139**, 109988 (2020). https://doi.org/10.1016/j.eurpolymj.2020.109988

[62] Ghasemlou M., Daver F., Ivanova E. P., Brkljaca R., Adhikari B.: Assessment of interfacial interactions between starch and non-isocyanate polyurethanes in their hybrids. Carbohydrate Polymers, **246**, 116656 (2020). https://doi.org/10.1016/j.carbpol.2020.116656

[63] Janvier M., Ducrot P-H., Allais F.: Isocyanate-free synthesis and characterization of renewable poly(hydroxy) urethanes from syringaresinol. ACS Sustainable Chemistry and Engineering, **5**, 8648–8656 (2017). https://doi.org/10.1021/acssuschemeng.7b01271

[64] Liu H., Li S., Wang M., Liu H., Jiang J., Shao S., Wang Z.: Toughened polybenzoxazine coating matrix with improved comprehensive performance through hydrogen bond tuning with new polyurethanes. Progress in Organic Coatings, **180**, 107555 (2023). https://doi.org/10.1016/j.porgcoat.2023.107555

[65] Mosikatsi B. E., Mabuba N., Malinga S. P.: Thin film composite membranes consisting of hyperbranched polyethylenimine (HPEI)-cysteamine layer for cadmium removal in water. Journal of Water Process Engineering, **30**, 100686 (2019). https://doi.org/10.1016/j.jwpe.2018.10.004

[66] Porto D. S., de Faria C. M. G., Inada N. M., Frollini E.: Polyurethane films formation from microcrystalline cellulose as a polyol and cellulose nanocrystals as additive: Reactions favored by the low viscosity of the source of isocyanate groups used. International Journal of Biological Macromolecules, **236**, 124035 (2023). https://doi.org/10.1016/j.ijbiomac.2023.124035

[67] John B., Rajimol P. R., Rajan T. P. D., Sahoo S. K.: Design and fabrication of nano textured superhydrophobic and anti-corrosive silane-grafted ZnO/bio-based polyurethane bilayer coating. Surface and Coatings Technology, **451**, 129036 (2022). https://doi.org/10.1016/j.surfcoat.2022.129036

[68] Liang D., Wang Y., Shi H., Luo Z., Quirino R. L., Lu Q., Zhang C.: Controllable release fertilizer with low coating content enabled by superhydrophobic castor oil-based polyurethane nanocomposites prepared through a one-step synthetic strategy. Industrial Crops and Products, **189**, 115803 (2022). https://doi.org/10.1016/j.indcrop.2022.115803